Method for Quantitative Evaluation of Kinetic Constants in Olefin Polymerizations. II. Kinetic Study of a High-Activity Ziegler–Natta Catalyst Used for Bulk Propylene Polymerizations

Válter Matos,[1] Antônio G. Mattos Neto,[1] Márcio Nele,[2] José Carlos Pinto[2]

[1]*Polibrasil Resinas SA, Rua Hidrogênio, 1404, Complexo Petroquímico de Camaçari, Camaçari, 42810-000 BA, Brazil;* [2]*Programa de Engenharia Química/COPPE, Universidade Federal do Rio de Janeiro, Cidade Universitária, CP:68502, Rio de Janeiro, 21945-970 RJ, Brazil*

Received 13 April 2001; accepted 24 January 2002

ABSTRACT: A method for quantitative evaluation of kinetic constants in Ziegler–Natta and metallocene olefin polymerizations presented previously (Matos, V.; Mattos Neto, A. G.; Pinto, J. C. J Appl Polym Sci 2001, 79, 2076) is adapted to allow the estimation of kinetic constants for bulk propylene polymerizations by using a conventional fourth-generation high-activity Ziegler–Natta catalyst (HAC). In this particular case, reaction rate profiles are not available, so that estimation of kinetic data must rely on average polymer yields. The method comprises some fundamental steps, including the initial design of a statistical experimental plan, the execution of the designed experiments, the development of simple mathematical models to describe the polymerization, and the estimation of kinetic parameters from available yields, gel permeation chromatography (GPC), and nuclear magnetic resonance (NMR) data. It is shown that the proposed method allows the successful interpretation of experimental olefin polymerization data and the quantitative evaluation of kinetic parameters, which can be inserted into a process simulator to provide an accurate picture of actual industrial plant behavior. © 2002 Wiley Periodicals, Inc. J Appl Polym Sci 86: 3226–3245, 2002

Key words: Ziegler–Natta; catalyst; propylene; polymerization; estimation; kinetic constant; kinetic parameter

INTRODUCTION

Polyolefins may be regarded as the most important plastics produced in the world.[1] Although polyolefins have the largest market share in the plastic industry, the competition in this market is fierce with the regular announcement of new plants worldwide,[2] driving older plants to cut their operational costs to remain competitive. Besides, the polyolefin industry finds itself in a conflicting situation: although it is a commodity-based industry, there is an increasing market demand for polyolefins tailored to meet specific needs. The polyolefin producers that can answer to that demand can guarantee a market share with higher profits. Because of that, significant engineering activity is carried out in the polyolefin industry, related to design of new plants, cutting of costs in existing sites, and development of new products.

Very frequently, these engineering activities are carried out with the aid of commercial-process simulators such as Polyred (Hypro-tech), Polymers Plus (Aspen), Pro II (Simulation Science), and Simulpol[3] (COPPE/Polibrasil). There also is significant academic effort to model olefin polymerization reactors.[4–8] In addition to well-founded reactor models, reliable kinetic parameters are essential to the proper use of these simulators/models. If fair estimates of the kinetic parameters are not available, engineers have to rely on rough guesses, which may lead to unwanted uncertainties in the decision-making process and may certainly make process simulation useless.

The estimation of sound kinetic parameters in Ziegler–Natta polymerization is a difficult task. Ziegler–Natta systems comprised multiple active sites, multiple chain transfer agents, and catalyst decay allied to the significant variability of catalyst behavior due to different preparation methods[9] and the high sensitivity to impurities, namely, oxygen and moisture. The literature presents very few kinetic studies about Ziegler–Natta polymerizations, and most of them focus on specific aspects of the system.[10] Besides, available studies are carried out at low pressures in diluent, hindering the use of the kinetic parameters presented on real-world problems where the polymerizations are carried out at high pressures, or in liquid monomer.

Correspondence to: J. C. Pinto (pinto@peq.coppe.ufrj.br).
Contract grant sponsor: Polibrasil Resinas SA.

In particular, modern polyolefin processes such as the ones constituted by loop reactors[11] and liquid pool reactors[12] are carried out by using fourth-generation Ziegler–Natta catalysts in liquid monomer at high pressures. Nevertheless, the only kinetic studies of fourth-generation Ziegler–Natta catalysts in liquid propylene seem to be the ones performed by Weickert and coworkers.[13,14] In these articles, kinetic models are developed for reaction rates and very detailed studies of the effect of cocatalysts and hydrogen on the polymerization yield, induction time, initial reaction rate, and decay rate are performed at a fixed temperature (42°C).

When performed in bench-scale reactors, the operation of high-pressure bulk propylene polymerizations may be very different from the operation of slurry polymerizations. The main difference for parameter estimation purposes, though, regards the evaluation of the reaction rate data. In slurry polymerizations, continuous monomer consumption inside the reactor provides the driving force for continuous monomer feed from a storage vessel, which can be measured in-line. In bulk polymerizations, the liquid monomer keeps the reaction pressure constant throughout the polymerization, so that in-line evaluation of reaction rate is much more difficult, and in some cases, economically impossible.

In-line calorimetry[15] might be used to keep track of the reaction rates during the reaction batch if the fouling of the reactor wall is negligible and the heat losses are small, although it is almost impossible to avoid significant heat losses in small lab-scale reactors. Thus, most of time one has to rely on the final polymer yields to evaluate the performance of the process catalysts. In this case, the method previously developed[10] for estimation of kinetic parameters has to be adapted for the case where reaction rate profiles are not available.

The main objective of this article is to adapt the method for quantitative evaluation of kinetic parameters developed earlier[9] to allow the detailed kinetic investigation of the bulk propene polymerization with a fourth-generation Ziegler–Natta catalyst (HAC). Based on a simple multisite kinetic mechanism used to describe the polymerization reaction, kinetic parameters are estimated for the propagation, decay, and transfer rates and also for the catalyst stereoselectivity to provide a consistent set of kinetic constant suitable to the use in process simulation. The set of kinetic data obtained is then inserted into SIMUPOL to simulate a liquid pool process. Simulation results are compared to actual plant data and it is shown that the observed agreement may be regarded as excellent.

EXPERIMENTAL

Catalyst preparation

Catalyst is provided as a solid suspension in mineral oil, containing about 40% of solids in mass basis. For proprietary reasons, detailed description of catalyst preparation procedure and catalyst properties cannot be presented here. However, it is important to say that the catalyst is composed of $TiCl_4$ crystals over a porous magnesium dichloride ($MgCl_2$) material and it contains ethyl benzoate (EB) as the internal donor. The final catalyst titanium content is ~ 3% in mass basis. Figure 1(a, b) shows typical particle-size distributions for the catalyst particles. It may be observed that catalyst particles present broad particle-size distribution. The catalyst is used in conjunction with ethyl *p*-ethylbenzoate (PEEB) as the external donor and alquil aluminums [triethyl aluminum (TEA) and diethylaluminum chloride (DEAC)] as cocatalysts. The catalyst was a commercial sample kindly offered by a catalyst manufacturer. TEA, DEAC, and PEEB were provided by Akzo Nobel, São Paulo-SP, Brazil.

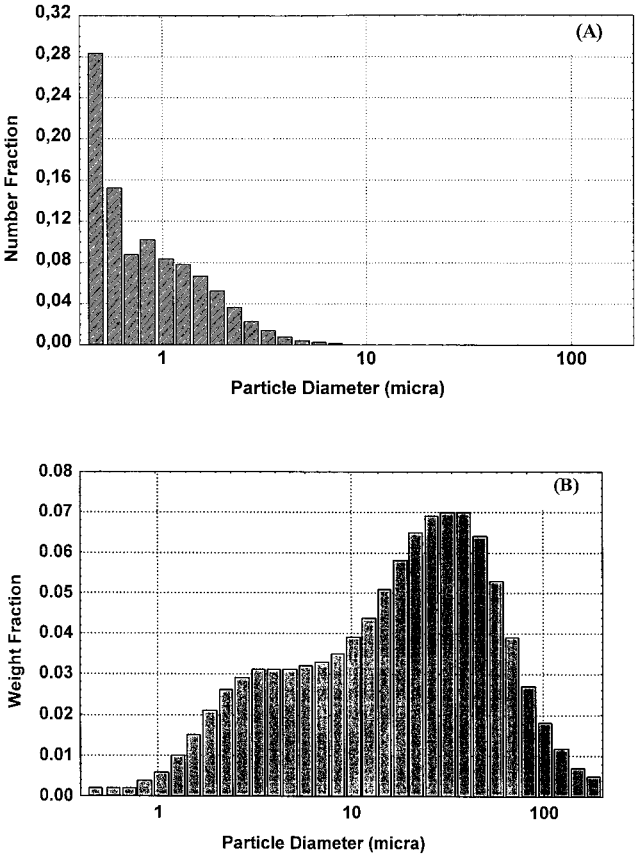

Figure 1 Typical particle size distribution (a) and morphology (b) obtained for catalyst powder.

Polymerization reaction

Polymerization reactions are carried out in a standard 2-L stainless steel Paar reactor, equipped with internal coils for refrigeration and temperature control. The reaction mixture is stirred continuously with a speed-controlled stirrer equipped with a three-blade turbine impeller. Heat is provided by an external heating

mantle. Reactor temperature and pressure are monitored and controlled in-line. The propylene feed line is equipped with a mass flow meter (Aalborg), which measures propylene feed rates continuously. All reaction variables are stored in a standard PC process computer, which is connected with the reactor instruments through a data acquisition board (Strawberry). Data acquisition and control algorithms are implemented with the software *Workbench 3.0* (Strawberry), which manipulates the data acquisition board.

Before reaction is started, the reactor is blown with nitrogen (high-purity polymerization grade provided by COPENE, Camaçari-BA, Brazil) to remove oxygen and humidity. The reactor is then charged with 1 L liquid propylene (high-purity polymerization grade provided by COPENE) under nitrogen atmosphere, at ambient temperature. Afterwards, temperature is increased slowly to the desired reaction temperature. After temperature stabilization, the reactor is vented for $\sim$ 30 s to remove the nitrogen excess and other volatile species. After new temperature and pressure stabilization, hydrogen (99.5% pure polymerization grade, provided by White Martins, Camaçari-BA, Brazil) is fed into the reactor vessel at constant temperature, until the final reaction pressure (or hydrogen partial pressure) is reached. After hydrogen addition, the desired amount of the first cocatalyst $AlEt_3$ (TEA) is fed as a solution in mineral oil containing 15% in mass of cocatalyst. Then, the desired amount of the second cocatalyst [*para*-etoxy-etyl-benzoate (PEEB)] is fed as a solution in mineral oil containing 15% in mass of cocatalyst. Finally, the desired amounts of the catalyst and of the third cocatalyst $AlClEt_2$ (DEAC) are fed as a suspension in mineral oil containing about 1% of solids. The cocatalyst solutions and the catalyst suspension are fed into the reactor vessel with a high-precision pneumatic metering pump (Polibrasil).

As soon as catalyst is added, reaction is assumed to begin. Reaction is then carried out for the specified batch time. After reaching the desired reaction time, polymerization is halted through fast and continuous gas venting of the reaction vessel (it generally takes a couple of minutes to reach ambient pressure). The reactor is opened and the solid material is collected, weighed, and characterized.

Polymer characterization

The polymer characterization procedures used in this work are the polymer fraction that is soluble in hot xylene (XO), the gel permeation chromatography (GPC), and the nuclear magnetic resonance(NMR) analysis.

The XO analysis is generally used to allow a rough evaluation of the total atactic, or moderately isotactic with low molecular weight, polypropylene (PP) content of the polymer resin. First, 2 g of polymer is dissolved in 100 mL boiling xylene (Aldrich, São Paulo-SP, Brazil), under continuous agitation. The solution is then left at boiling conditions for around 15 min. Afterwards, the solution is cooled down to 25°C. After 30 min resting, the solution is filtered. The solid and liquid phases are then dried under vacuum. The solid residual of the liquid phase (*XO*) and the solid powder (*insolubles*) are then weighed and characterized through GPC and NMR.

The GPC analysis was carried out in a Waters-150CV chromatograph, equipped with four Ultrastyragel separation columns (10^3-10^4-10^5-10^6) from Waters. Polymer samples were dissolved in 1,2,4-trichlorobenzene (TCB, Aldrich, São Paulo-SP, Brazil) and measurements were performed at 140°C. Polystyrene standards from polymer were used to calibrate the GPC instrument.

The ^{13}C-NMR analyses were carried out in Bruker Avance 500 equipment at frequencies of 125 MHz. The time interval used for each pulse was equal to 10 s. Polymer samples were dissolved in TCB and measurements were performed at 95°C. Deuterated benzene (Aldrich, São Paulo-SP, Brazil) was added to the polymer solution to allow the homogenization of the magnetic field and to improve the resolution of the spectral analysis. Polymer characterization was based on the methyl (CH_3, 20–22 ppm) and methylenic (CH_2, 45–47 ppm) signals, as described in the literature.[16,17]

Experimental design

Statistical design of experiments allows one to study the effects of all independent experimental variables at the same time, instead of the traditional method of one variable at a time, so that the effects of all independent variables can be quantified.

Seven independent variables related to the polymerization process were selected for this study. The first variable is the hydrogen concentration in reactor head ($0 < x_H < 7\%$), which is a very important variable[18,19] to the polymer molecular weight and the catalyst productivity. The second variable is the reactor temperature, which is allowed to vary within the interval $60 < T < 70$°C. The third variable is the catalyst concentration, evaluated as the total amount of titanium added to the reactor vessel ($40 < TiCl_4/MgCl_2 < 60$ ppm). The fourth variable is the batch time ($0.5 < t < 1.5$ h), included in the experimental design to allow the evaluation of the well-known catalyst decay.[20] The fifth variable is the amount of TEA added to the reaction environment during polymerization, evaluated in ppm ($40 < TEA < 70$ ppm). The sixth variable is amount of DEAC used in the precontact with the catalyst, evaluated in ppm ($12 < DEAC < 33$ ppm). The seventh variable was the external electron donor (PEEB) concentration, evaluated in ppm ($53 < PEEB < 65$ ppm) and known to influence the catalysts ste-

TABLE I
Experimental Design and Experimental Results

Label	T (°C)	t (h)	x_H (%)	Cat (ppm)	TEA (ppm)	DEAC (ppm)	PEEB (ppm)	Y (g)	Efic (gPo/gCat)	XO (% w/w)	PM_w (kDa)
H1	60	0.5	0.0	40.0	40.0	13.0	53.0	44	5500		865
H1	60	0.5	0.0	40.2	40.2	13.1	53.3	45	5603	5.30	
H2	60	0.5	0.0	60.2	70.2	33.0	65.2	136	11,295	7.89	730
H2	60	0.5	0.0	60.2	70.2	33.0	65.2	138	11,461		
H3	60	1.5	7.0	40.7	40.8	33.6	66.0	125	15,356	4.96	396
H3	60	1.5	7.0	39.8	39.8	32.8	64.6	140	17,610		
H4	60	1.5	7.0	59.8	69.9	13.0	53.0	257	21,506	7.26	395
H4	60	1.5	7.0	60.0	70.0	13.0	53.0	264	22,018		
H5	70	0.5	7.0	40.6	71.0	13.2	65.8	104	12,823	3.86	313
H5	70	0.5	7.0	40.0	70.0	13.0	65.0	97	12,125		
H6	70	0.5	7.0	60.1	40.1	33.0	53.2	181	15,058		202
H6	70	0.5	7.0	60.6	40.4	33.3	53.6	183	15,111	4.61	
H7	70	1.5	0.0	40.0	70.1	33.0	53.2	181	22,625	6.21	600
H7	70	1.5	0.0	40.1	70.0	33.0	53.0	181	22,596		
H8	70	1.5	0.0	60.6	40.4	13.2	65.6	21	1734		
H8	70	1.5	0.0	59.8	39.7	13.0	65.0	21	1755	5.49	977
H9	65	0.5	3.5	50.1	55.1	23.0	60.1	150	14,970		
H9	65	0.5	3.5	50.2	55.3	23.1	60.3	144	14,342	4.52	559
H10	65	1.0	3.5	50.1	55.1	23.0	60.1	173	17,265		555
H10	65	1.0	3.5	50.5	55.6	23.2	60.7	178	17,623	5.040	636
H11	65	1.5	3.5	50.4	55.4	23.1	60.5	221	21,946		603
H11	65	1.5	3.5	50.2	55.0	23.0	60.0	220	21,912	5.86	

reoselectivity.[21] The experimental ranges selected in all cases are in accordance with actual industrial operation conditions. The ranges are narrow on purpose, to allow the investigation of effects caused by variable fluctuations within usual operation constraints and must not be regarded as an experimental drawback.

To analyze the main effects of the selected variables upon the polymerization results, a minimum Taguchi experimental design[22] was proposed. The minimum Taguchi design allows the evaluation of main variable effects independently from each other, provided that variable interactions are not important. This is certainly a false assumption and the consequences of this assumption were discussed elsewhere.[9]

As in the first study,[9] all experiments were made in duplicate to allow the proper evaluation of experimental error. The most expensive analysis, however, was carried out only for a smaller subset of the whole experimental set. Additional central experiments were added to the experimental plan to allow the evaluation of possible nonlinear effects. Central experiments were performed for three distinct batch-time levels to verify whether the catalyst decay would exert any significant effect upon experimental reproducibility.

All experiments were executed at random. Experimental conditions and results obtained are shown in Table I. The experimental responses selected were polymerization yield (Y) in grams, catalyst efficiency (Efic) in grams of polymer per gram of catalyst, polymer fraction soluble in xylenes (XO) in % w/w, the polymer weight-average molecular weight (PM_W) in kDa, and the GPC curves and NMR spectra. Activity curves for some reference polymerization conditions were carried out in diluent (isododecane) to investigate the kinetics of catalyst decay qualitatively. XO values were not evaluated for all polymer samples because of the high costs of the XO analysis (XO analysis is too long), but at least one value is available for each experimental condition. Such experimental constraints are very common in an industrial lab and the experimental strategy must be flexible enough to accommodate possible lack of data.

DATA ANALYSIS

The first important piece of information that can be obtained from the experimental data presented in Table I is the experimental error in the catalyst evaluation. According to Table II, the standard deviation for

TABLE II
Linear Main Effect Analysis Between the Independent Experimental Variables and the Experimental Responses

	Y	XO	PM_W
b[a]	**146.68**	**5.556**	**566.2**
T	−11.02	**−0.655**	**−37.2**
t	**20.40**	0.364	**30.2**
x_H	**36.45**	−0.531	**−233.3**
Cat	**17.89**	**0.621**	16.1
TEA	**38.90**	**0.632**	**−52.4**
DEAC	**26.47**	0.225	**−80.2**
PEEB	**−34.64**	−0.190	**49.6**
r^2	0.86	0.94	0.99

[a] Independent term of the linear regression.

polymer yield is equal to 6 g, which means that polymer yield is accurate within ±20 g with confidence of about 95%. Previous study[10] showed that the accuracy of the XO and molecular weight determination is within ±0.60 and ± 0.25%, respectively, with confidence of about 95%. These numbers are very important because they will be used for analysis of model adequacy and statistical significance in the following subsections. Typical output values for polymer yield and XO are 150 ± 20 g and 5.53 ± 0.6%, respectively, with confidence of 95%.

TABLE III
Linear Main Effect Analysis Between the Relevant Catalyst Ratios, Independent Experimental Variables, and Experimental Responses

	Efic	*XO*	PM_W
b[a]	**15633**	**5.56**	**548**
T	−126	−0.51	**−44**
t	**1636**	0.24	**50**
x_H	**3053**	−0.53	**−233**
$r_{DEAC/Ti}$	**4385**	0.19	**−116**
$r_{TEA/PEEB}$	**7202**	**1.65**	**−123**
$r_{TEA/Ti}$	−2402	−1.21	60
r^2	0.85	0.85	0.99

[a] Independent term of the linear regression.

Influence of process conditions

The main effect analysis is carried out by building multiple linear models that relate the experimental responses (e.g., polymerization yield) with the independent experimental variables (e.g., cocatalyst concentration). The model coefficient on the independent variables is called the variable "effect," and this effect is said significant if it is larger than the experimental error. Table II shows the regression coefficients of these multiple linear models representing the experimental responses and the normalized [+1, −1] independent experimental variables, or alternatively, the main linear effects among the variables analyzed (the 95% significant effects are printed in bold).

Reaction temperature is usually the most important variable. However, within the experimental space investigated, its effect is only statistically significant for the polymer molecular weight, following the usual inverse relation between reaction temperature and polymer molecular weight. There is also a trend of decreasing XO as the reaction temperature increases. This effect is the inverse of the expected trend and can be tentatively attributed to the multisite character of the catalyst, as discussed later, as the catalyst is composed of multiple active sites with different responses to changes in the reaction temperature.

As expected, an increase in the catalyst amount and the reaction time provokes a proportional increase in the reaction yield. The catalyst amount also influences the XO fraction by changing the cocatalysts to titanium ratios in the reaction system.

The reaction time increases the reaction productivity, the polymer molecular weight, and the polymer XO fraction. Although the increase in the yield is in the expected direction, the influence in the polymer molecular weight and XO fraction can only be rationalized by evoking the multisite character of the catalyst. Different sites may have different decay rates[10] and the final polymer properties may depend on the reaction time.

The effect of both alquil aluminums (TEA and DEAC) are similar in trend. The activation of the catalyst sites and the reaction medium scrubbing by them lead to an increase in the catalytic activity. However, this activation is not selective because there also is an increase in the XO fraction with the increase in the TEA concentration, probably related to some extent to the interaction between TEA and PEEB discussed in more detail later. The alquil aluminums (TEA and DEAC) also show a similar effect on the polymer molecular weight, acting as chain-transfer agents.

The external electron donor (PEEB) decreases the catalyst activity by coordinating to active catalyst sites, poisoning selectively sites that produce low molecular weight PP, increasing the final polymer molecular weight.

The hydrogen concentration is the most important experimental variable for the reaction yield and polymer molecular weight. Although hydrogen activates dormant sites, it is also the most important chain-transfer agent and should be carefully controlled at plant sites.

In summary, in the experimental space investigated (closely related to the plant operational conditions), the polymer yield is strongly influenced by the hydrogen, TEA and PEEB concentration, and to a lesser extension by the DEAC concentration. Hydrogen concentration is also the most important variable to the molecular weight control, although fluctuations of cocatalyst concentrations may disturb the control of this variable at plant site. The XO fraction is very stable in relation to the experimental variables; however, it shows a direct correlation with TEA and catalyst concentrations, certainly related to the aluminum to titanium and aluminum (especially from TEA) to PEEB ratios.

In addition to concentrations, this system may be influenced by the catalyst component ratios. The main effect analysis was then carried out by transforming concentrations in molar ratios. The new independent variables related to the catalyst system are then DEAC to catalyst ratio ($r_{DEAC/Ti}$), TEA to catalyst ratio ($r_{TEA/Ti}$), and the TEA to PEEB ratio ($r_{TEA/PEEB}$). The results of the main effect analysis are presented in Table III.

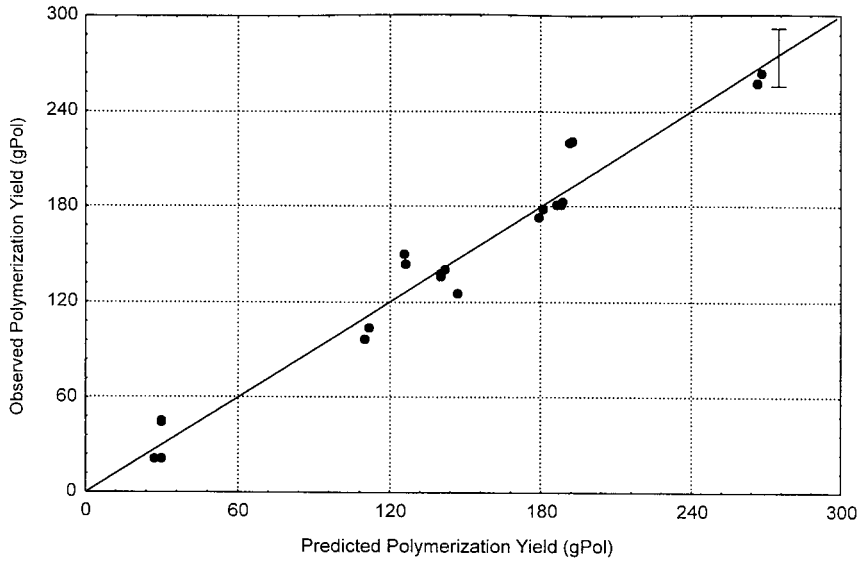

Figure 2 Comparison between predicted and observed polymerization yield using the empirical model.

The results in Table III show that the TEA/PEEB ratio has a very strong effect upon the catalyst efficiency within the experimental region investigated (TEA/PEEB = 0.4 to 1.0). A similar effect was observed by Weickert et al.,[14] who observed that PEEB affects both catalyst initial activity, by instantaneously poisoning catalyst active sites, and catalyst decay. Within these TEA/PEEB ratios, TEA decreases the poisoning power of the PEEB by complexing preferentially with the strong electron-releasing carbonyl group,[1] so that the catalyst efficiency increases as the TEA/PEEB ratio increases. The effect of the TEA/PEEB ratio on the XO fraction is remarkable. It is the only statistically significant variable and the XO fraction increases as the TEA/PEEB ratio increases because of the combined effect of poisoning the low stereoselectivity sites by PEEB and the complexation of TEA and PEEB. Therefore, as the TEA content increases, the PEEB has its poisoning power reduced by TEA and a smaller number of low stereoselectivity sites are able to produce XO-soluble PP. The increase in the TEA/PEEB ratio also leads to the decrease of the polymer average molecular weight. Two effects are envisaged here: the decrease of M_w due to the increase of the ratio of chain transfer to TEA and the increase of M_w due to the selective poisoning active sites that produce low molecular weight PP by PEEB. The ratio DEAC/Ti also influences the polymer molecular weight by the increasing of the rate transfer to DEAC, and the catalyst efficiency by activating the catalysts sites. Although the TEA is able to activate the catalyst (Table III), the ratio of TEA/Ti seems not to have much importance when compared to the other experimental variables, in the experimental region investigated, on all experimental responses. Similarly, very weak effects by TEA/Ti ratio were observed by Weickert et al..[14]

Semiempirical models based on physical reasoning, as performed previously,[2] were carried successfully only to polymerization yield, as shown in eq. (1) (r^2 = 0.96) and Figure 2. Attempts to develop such models to XO led to results that were much poorer than the ones obtained with the multiple linear regression performed before

$$Y = e^{(-1968.1/T)}e^{-0.680t}t(53.57\sqrt{\text{TEA}} + 44.97\sqrt{\text{DEAC}} - 58.58\sqrt{\text{PEEB}} + 41.92\sqrt{x_H}) \quad (1)$$

Analysis of polymerization rate profiles in diluent medium

Because of the nature of the bulk polymerization process and of our experimental setup, it is not possible to obtain instantaneous reaction rate data. However, it is very important to the process engineer to know the catalyst behavior over a period of time to evaluate the consequences of the catalyst deactivation. To provide this information, two slurry polymerizations were performed in an aliphatic hydrocarbon (isododecane-pentamethyl-heptane) at the central point experimental conditions, with different hydrogen concentrations (Fig. 3). The hydrogen concentration exerted a significant effect upon the polymer molecular weight, but, in this case, its effect on the polymer productivity was negligible (Table IV). The polymerization rate profiles (Fig. 3) show that hydrogen accelerates both the activation and the decay processes. Figure 3 also shows that the catalyst decay is very fast. The maximum polymerization rate is attained within 5 min of reaction, and the polymerization rate is almost negligible 20 min after start-up.

Based on the previous observations and the hypothesis that the polymerization conditions are held con-

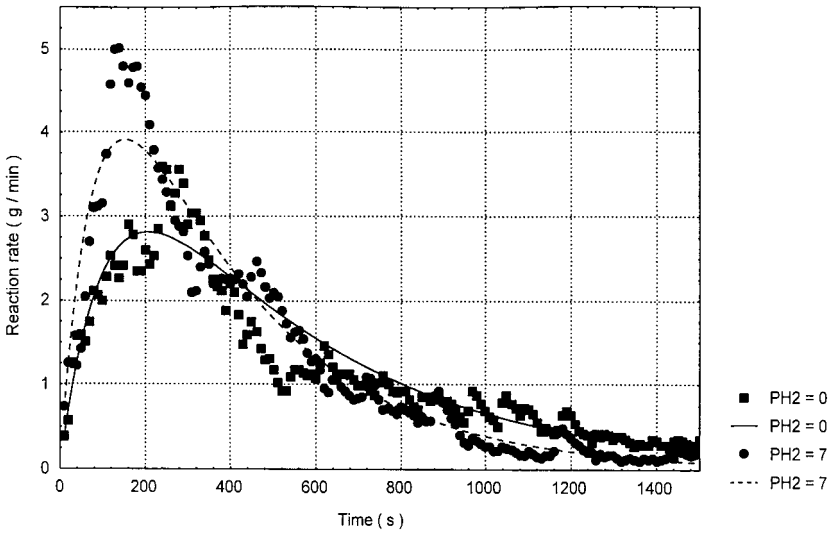

Figure 3 Comparison between predicted and observed catalyst rate using the complete model (polymerization in diluent, conditions in Table III).

stant throughout the experiment and that the catalyst is composed of N different active sites, the following kinetic scheme can be devised as a first approach:

$$M_i^0 \xrightarrow{K_{ri}} M_i^{at}$$

$$M_i^{at} + M \xrightarrow{K_{pi}} M_i^{at} + P$$

$$M_i^o \xrightarrow{K_{di}} M_i^d$$

$$M_i^{at} \xrightarrow{K_{di}} M_i^d \qquad (2)$$

where M_i^o is a potential catalyst site of type i; M_i^{at} is an active catalyst site of type i; M is the monomer species; M_i^d is a deactivated catalyst site of type i; and K_{ri}, K_{pi}, and K_{di} are the rate constants for site activation, chain propagation, and site deactivation reactions for site i, respectively.

The catalyst sites can be activated spontaneously or by external agents (e.g., hydrogen) as well as deactivated during the course of the polymerization. Therefore, the amount of dormant active sites during a batch can be described by:

$$\frac{dM_i^0}{dt} = -(K_{ri} + K_{di})M_i^0 \qquad (3)$$

$$M_i^0 = M_i^0(0)\exp[-(K_{ri} + K_{di})t] \qquad (4)$$

where the constants K_{ri} and K_{di} depend on the polymerization conditions.

The amount of active sites during a batch can be written in the following form:

$$\frac{dM_i^{at}}{dt} = K_{ri}M_i^0 - K_{di}M_i^{at} \qquad (5)$$

$$M_i^{at} = [\exp(-K_{di}t) - \exp(-(K_{ri} + K_{di})t)]M_i^0(0) \qquad (6)$$

Consequently, the instantaneous polymerization rate can be written as

$$\text{Rate} = \sum_{i=1}^{N} K_{pi}pMM_i^{at} = \sum_{i=1}^{N} K_{pi}f_i[\exp(-K_{di}t) - \exp(-(K_{ri} + K_{di})t)]pM\,Mcat \qquad (7)$$

TABLE IV
Experimental Conditions and Results for the Hydrogen Effect Study

Label	T (°C)	t (h)	x_H (%)	Cat (ppm)	TEA (ppm)	DEAC (ppm)	PEEB (ppm)	Y (g)	Efic (gPo/gCat)	XO (% w/w)	PM_w (kDa)
D1	65	1.0	7	27.2	74.9	31.2	81.8	43	1579	1.3	310
D2	65	1.0	0	27.5	75.7	31.6	82.6	43	1563	1.7	742

where f_i represents the fraction of sites i in the catalytic system, pM is the monomer partial pressure, and $Mcat$ the mass of catalyst added to the reactor.

Equation (7) can be directly used for reaction rate data interpretation and parameter estimation; however, it is more convenient to use its simpler asymptotic forms. At the limit when time goes to zero, eq. (7) can be written in the following asymptotic form:

$$\text{Rate} \approx \sum_{i=1}^{N} K_{pi} f_i K_{ri} t \; pM \; Mcat = A_1 t \tag{8}$$

where

$$A_1 = \sum_{i=1}^{N} K_{pi} f_i K_{ri} pM \; Mcat \tag{9}$$

At the limit where time goes to infinity, eq. (7) can also be written in the following asymptotic form:

$$\text{Rate} \approx \sum_{i=1}^{N} K_{pi} f_i \exp(-K_{di} t) pM \; Mcat \tag{10}$$

By using eq. (8) and the instantaneous reaction rate data obtained for reaction times < 150 s, it is possible to estimate the activation parameters A_1 to be equal to 84.02 (g/min) h^{-1} ($r^2 = 0.85$) and 127.00 (g/min) h^{-1} ($r^2 = 0.97$) for the reactions carried out in the absence and in the presence of hydrogen, respectively. Therefore, the initial catalytic activity increases about 50% in the presence of hydrogen.

By using eq. (10) and the instantaneous reaction rate obtained 400 s after the reaction start-up, it is possible to estimate the deactivation parameters in the following form:

$$\text{Rate} = 5.56 \exp(-7.81t) \tag{11}$$

for the reaction without hydrogen ($r^2 = 0.97$) and

$$\text{Rate} = 8.47 \exp(-11.01t) \tag{12}$$

for the reaction with hydrogen ($r^2 = 0.98$). In eqs. (11)-(12), reaction rates are described in g/min and time is in hours. It is interesting to note that within the experimental range investigated the presence of hydrogen promotes an increase in the maximum catalyst activity (preexponential factor) while increasing the rate of catalyst decay (exponential term). Similar results were obtained by Weickert et al.[14]

The estimated parameters can be combined to allow the computation of the entire rate curves. Equation (7) may be rewritten in the following form

TABLE V
Kinetic Parameters Estimated for the Polymerizations Carried Out in Diluent Medium

	$x_H = 0$	$x_H = 7$
A_1 [(g/min) h^{-1}]	144.37	270.78
K_r (h^{-1})	24.90	32.38
K_d (h^{-1})	7.81	11.01
r^2	0.97	0.95

$$Taxa = \frac{A_1}{K_r}\left[\exp(-K_d t) - \exp(-(K_r + K_d)t)\right] \tag{13}$$

where A_1 and K_d are the kinetic constants used to describe the catalyst as a single-site catalyst. Table V shows the final kinetic parameters obtained and Figure 3 illustrates the model performance.

It is important to mention that the increase of the number of catalytic sites did not improve the model fitting significantly, which may imply that steps of active site activation and decay depends weakly on the nature of the catalyst sites. It is also important to note the accelerating effect of hydrogen on all steps of the proposed kinetic scheme, which must be taken into consideration during the characterization of the catalyst performance in the following sections.

Analysis of the yield data in liquid pool polymerization

Based on the previous discussion, eq. (2) is used to describe the system behavior. The only additional hypothesis is that different active sites are activated by different chemical species. It is well known that a single chemical species (e.g., cocatalysts) can activate different catalyst sites, so that the division of the catalyst sites by the chemical species responsible for its activation may seem somewhat arbitrary. Nevertheless, this may be very useful for process-simulation purposes, as one can easily identify the effects of the different chemical species on the reactor yield. Therefore, the model takes the following form:

$$\text{Rate} = \frac{dP}{dt} = \sum_{i=1}^{N} K_{pi} pM \, M_i^{at} = \sum_{i=1}^{N} K_{pi} f_i [\exp(-K_{di} t) - \exp(-(K_{ri} X + K_{di})t)] pM \; Mcat \tag{14}$$

where X represents the chemical species responsible by the site activation. If $X = 1$, the activation is spontaneous. It is important to mention that many factors may be responsible for site activation.[23] In this case, the term that describes the catalyst activation is a weighed sum of all these factors.

To obtain the polymerization yield, eq. (14) must be integrated as

TABLE VI
Kinetic Parameters Estimated for the Polymerizations Carried Out in Liquid Propylene

Parameters	Values for eq. (20)	Values for eq. (21)
A	2.860	14.214
E_A	1977	−5467
K_d	1.957	4.070
K_h	—	0.229
Kx_{11}	3.525	1.999
Kx_{12}	2.961	1.901
Kx_{21}	2.776	—
Kx_3	3.852	2.236
r^2	0.96	0.94

$$Y = \sum_{i=1}^{N} K_{pi} f_i \left[\left(\frac{1 - \exp(-K_{di}t)}{K_{di}} \right) - \left(\frac{1 - \exp(-(K_{ri}X + K_{di})t)}{(K_{ri}X + K_{di})} \right) \right] pM\,Mcat \quad (15)$$

It is still convenient to modify eq. (15) by assuming that certain dormant sites are instantaneously activated/deactivated by external chemical species that reaches concentration equilibrium and that can be described by equations similar to the ones used in isothermal adsorption, in the form

$$Y = \sum_{i=1}^{N} K_{pi} f_i \left[\sum_{j=1}^{NX} \left(\frac{X_j}{1 + Kx_{ij}X_j} \right) \right] \times \left[\left(\frac{1 - \exp(-K_{di}t)}{K_{di}} \right) - \left(\frac{1 - \exp(-(K_{ri}X + K_{di})t)}{(K_{ri}X + K_{di})} \right) \right] pM\,Mcat \quad (16)$$

where Kx_{ij} is the adsorption equilibrium constant of the species j on the site i and NX is the number of chemical species able to activate the active sites. Note that in this equation K_{pi} takes into account this constant.

Initially, eq. (16) was used to represent the polymerization yield data presented in Table I. The parameter estimation procedure was carried out in a stepwise fashion, starting from eq. (14) in its simplest form with only one active site, and then adding parameters as they were judged to be necessary. The objective criteria for adding a parameter was a gain of at least 5% in the correlation coefficient without any loss in the physical meaning of the parameters (negative or very large kinetic constants were discarded).

During the estimation procedure, eq. (16) was further simplified. The activation constant converged to very high values, suggesting that catalyst activation is very fast in liquid propylene. Therefore, in this case, eq. (16) can take the following form:

$$Y = \sum_{i=1}^{N} K_{pi} f_i \left[\sum_{j=1}^{NX} \left(\frac{X_j}{1 + Kx_{ij}X_j} \right) \right] \times \left(\frac{1 - \exp(-K_{di}t)}{K_{di}} \right) pM\,Mcat \quad (17)$$

Furthermore, the heat and mass transfer rates should be very efficient in liquid propylene, so that changes of monomer concentration and reaction temperature are expected to be very small throughout the polymerization. Therefore, eq. (17) may be rewritten in the form:

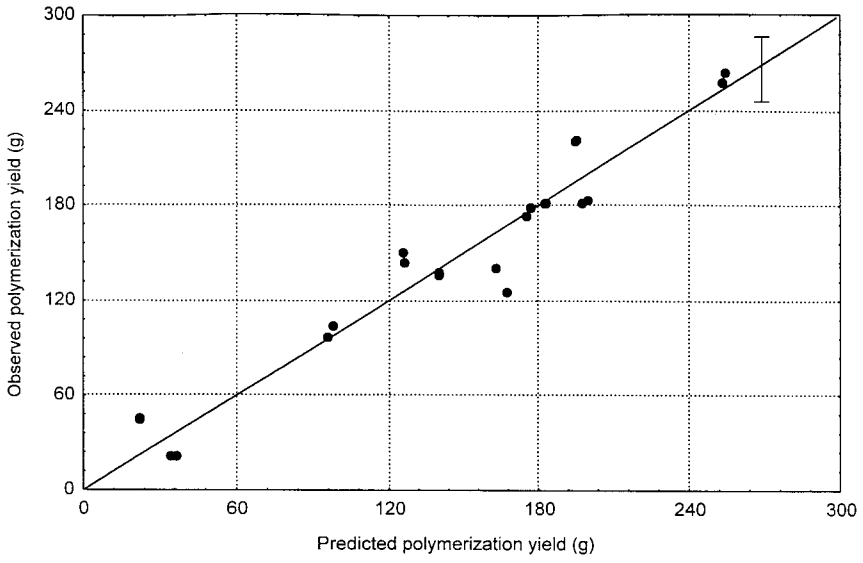

Figure 4 Comparison between predicted [eq. (20)] and observed polymerization yield.

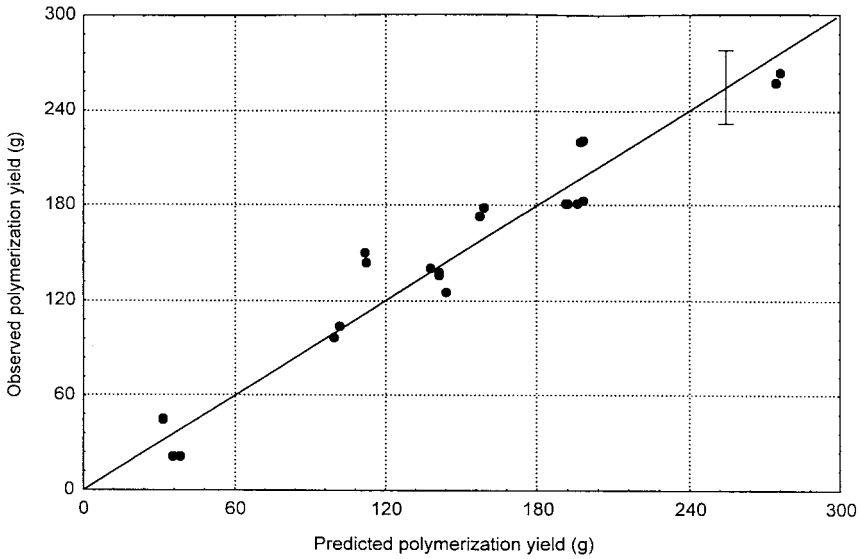

Figure 5 Comparison between predicted [eq. (21)] and observed polymerization yield.

$$Y = \sum_{i=1}^{N} (K_{pi} f_i) \left[\sum_{j=1}^{NX} \left(\frac{X_j}{1 + K x_{ij} X_j} \right) \right] \times \left(\frac{1 - \exp(-K_{di} t)}{K_{di}} \right) pM\, Mcat \quad (18)$$

where the lumped parameter is the one effectively estimated.

After implementation of the parameter estimation procedure, it was found that a Friedlish instead of a Langmuir[24] isotherm leads to an easier parameter estimation procedure. Therefore, eq. (18) takes the form:

$$Y = \sum_{i=1}^{N} (K_{pi} f_i) \left[\sum_{j=1}^{NX} \sqrt{X_j} \right] \left(\frac{1 - \exp(-K_{di} t)}{K_{di}} \right) pM\, Mcat \quad (19)$$

If we assume that the deactivation constant is the same for all active sites, and lump the dependence of the catalyst yield upon the temperature in the propagation rate constant, eq. (20) can be obtained (parameters on Table VI). It should be noted that the parameter effectively estimated is $e^{A} K x_{ij}^{p}$, and the superscript p refers to the productivity model [eq. (20)]. The correlation coefficient between experimental and calculated data was $r^2 = 0.96$, and the adequacy of the model can be assessed in Figure 4:

$$Y = \frac{e^{[A-(E_A/T)]}}{K_d} (1 - e^{-K_d t})(K x_{11}^{p} \sqrt{\mathrm{DEAC}} + K x_{12}^{p} \sqrt{\mathrm{TEA}} + K x_{21}^{p} \sqrt{x_H} - K x_3^{p} \sqrt{\mathrm{PEEB}}) pM\, Mcat \quad (20)$$

Some features of the model described by eq. (20) must be discussed. The minus sign on the adsorption coefficient of the PEEB takes into account the selective poisoning of active sites by reaction with the external electron donor. This effect agrees with experimental observation that the external donor selectively poisons low stereoselectivity catalyst sites.[21] The model predicts that the catalytic activity should increase as the hydrogen concentration in the reactor increases, as observed in the diluent polymerizations. Equation (20) also predicts an activation effect by DEAC and TEA. For process simulation purposes, one can say that the catalyst presents two distinct active sites, one activated by cocatalysts (TEA and DEAC) and a second one activated by hydrogen.

The masses of polymer produced by the sites activated by hydrogen and by cocatalysts, estimated by using eq. (20) at the central experimental conditions (H10 at Table I), are equal to 69.7 and 118.1 g, respectively. That means that about 37% of the polymer produced is due to the hydrogen activation effect. The possible causes for this effect are the activation of new catalyst sites or the re-activation of dormant sites by hydrogen.[18,19] It is pertinent to mention that it was not possible to lump both effects (hydrogen and cocatalyst) into a single polymer yield expression, which seems to reinforce the assumption of considering two different catalyst sites for simulation purposes.

If we assume that instead of activating new sites, hydrogen re-activates previously deactivated sites, rendered inactive by 2,1 insertions,[21] the expression for polymerization yield takes the form:

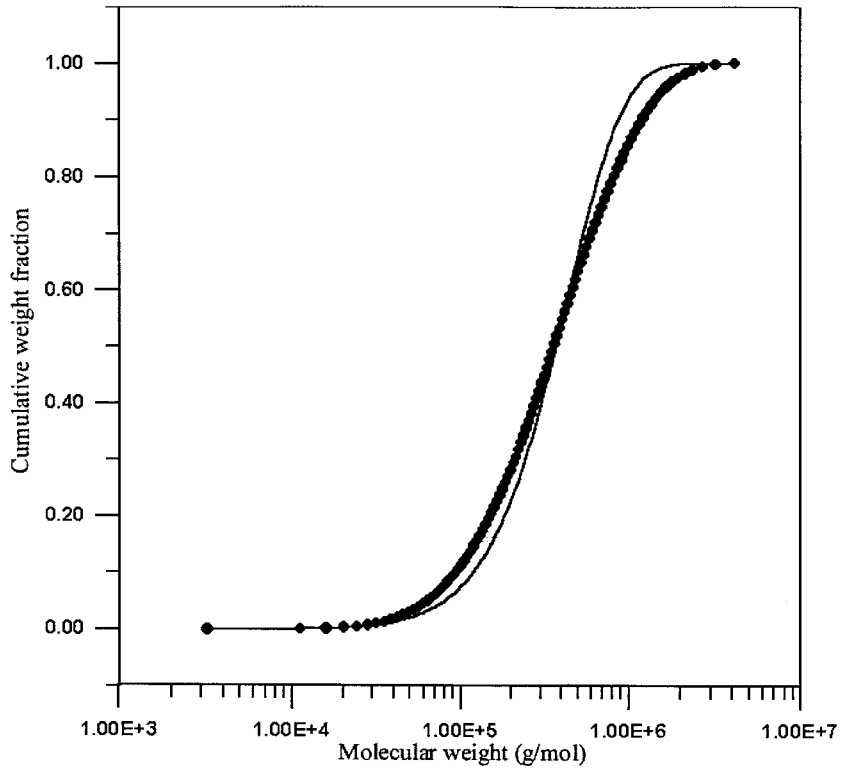

Figure 6 Deconvolution of the experimental MWD for polymerization H10, with the use of one catalyst site. (●, experimental; —, model).

$$Y = \frac{e^{[A-(E_A/T)]}}{(K_d^2 + K_h x_H)} [K_h^2 x_H^2 t + K_d(K_h x_H t + 1 - e^{-(K_d + K_h x_H)t})] \times (K x_{11}^p \sqrt{\overline{\text{DEAC}}} + K x_{12}^p \sqrt{\overline{\text{TEA}}} - K x_3^p \sqrt{\overline{\text{PEEB}}}) pM\, Mcat \quad (21)$$

Equation (21) describes the experimental data with approximately the same quality as eq. (20) does. The parameters are presented in Table VI, and the excellent fitting to the experimental data can be evaluated in Figure 5.

Therefore, both activation of new catalyst sites and the re-activation of dormant sites by hydrogen are able to describe the experimental data. The discrimination between the two effects is beyond the scope of this work, and eq. (20) was chosen to calculate catalyst activity-related data because it is simpler.

GPC deconvolution

Gel permeation chromatography provides a powerful tool for obtaining kinetic information. Detailed information may be obtained regarding the number of active sites, the ratio of transfer to propagation reaction rates for each site, and also the fractional contribution of each site for the total polymer productivity,

TABLE VII
Kinetic Parameters Estimated from GPC Curves and Averages of the Obtained MWD

Label	θ_1	θ_2	α_1	PM_n (kg/gmol)	PM_w (kg/gmol)	PD
H1	0.72×10^{-4}	2.57×10^{-4}	0.801	387	865	2.24
H2	0.92×10^{-4}	2.40×10^{-4}	0.777	337	730	2.17
H3	1.62×10^{-4}	4.52×10^{-4}	0.601	151	396	2.62
H4	1.66×10^{-4}	4.30×10^{-4}	0.609	156	395	2.53
H5	2.24×10^{-4}	4.22×10^{-4}	0.664	145	313	2.16
H6	—	3.73×10^{-4}	0.000	113	202	1.79
H7	1.04×10^{-4}	3.26×10^{-4}	0.665	235	600	2.56
H8	0.70×10^{-4}	2.82×10^{-4}	0.947	517	977	1.89
H9	1.11×10^{-4}	3.16×10^{-4}	0.613	221	559	2.53
H10	1.09×10^{-4}	3.64×10^{-4}	0.630	207	555	2.69
H11	0.98×10^{-4}	3.46×10^{-4}	0.637	224	603	2.69

TABLE VIII
Correlation and Linear Main Effect Analysis for the Parameters Obtained from GPC, the Independent Experimental Variables, and the Experimental PM_w and PD

	Correlation analysis			Linear effect analysis
	θ_1	θ_2	α_1	α_1
b[a]	—	—	—	**0.63**
T	0.07	0.04	−0.24	**−0.07**
t	−0.04	0.31	0.26	**0.06**
x_H	**0.86**	**0.86**	**−0.63**	**−0.17**
Cat	−0.29	−0.19	−0.20	**−0.05**
TEA	0.44	0.09	0.17	**0.05**
DEAC	−0.13	0.01	−0.46	**−0.13**
PEEB	0.23	0.03	0.41	**0.12**
PM_w	**−0.89**	**−0.79**	**0.79**	—
PD	0.13	0.27	0.20	—

[a] Independent term of the linear regression.

if the model hypotheses are satisfied. The main model hypotheses are as follows: (1) the catalyst is a mixture of a finite number of active sites; (2) each active site produces polymer with MWD that may be described by Schulz–Flory distribution; (3) the polymerization conditions are kept constant throughout the polymerization; and (4) there is no site transformation throughout the polymerization.

The mathematical modeling of GPC curves was discussed in detail in the previous work.[10] For the purposes of this work, it is sufficient to say that the polymer MWD is sum of Schulz–Flory distributions in the form:

$$\Lambda_i = \sum_{j=1}^{N} A_j q_j^{i-1} \tag{22}$$

where Λ_i is the molar concentration of polymer chains of size i in a polymer sample, A_j depends on the concentration of the catalyst site type j, and q_j is the propagation probability of catalyst site j and depends on the polymerization mechanism. If eq. (22) is normalized in relation to the total mass of polymer, and rewritten in terms of the mass fraction of polymer chains of size i, one obtains the cumulative molecular weight distribution as

$$F_L = \frac{\sum_{j=1}^{N} \alpha_j\{1 - q_j^L[1 + L(1 - q_j)]}{\sum_{j=1}^{N} \alpha_j} \tag{23}$$

where α_j is the relative activity of the catalyst site type j or the polymer mass fraction produced by the cata-

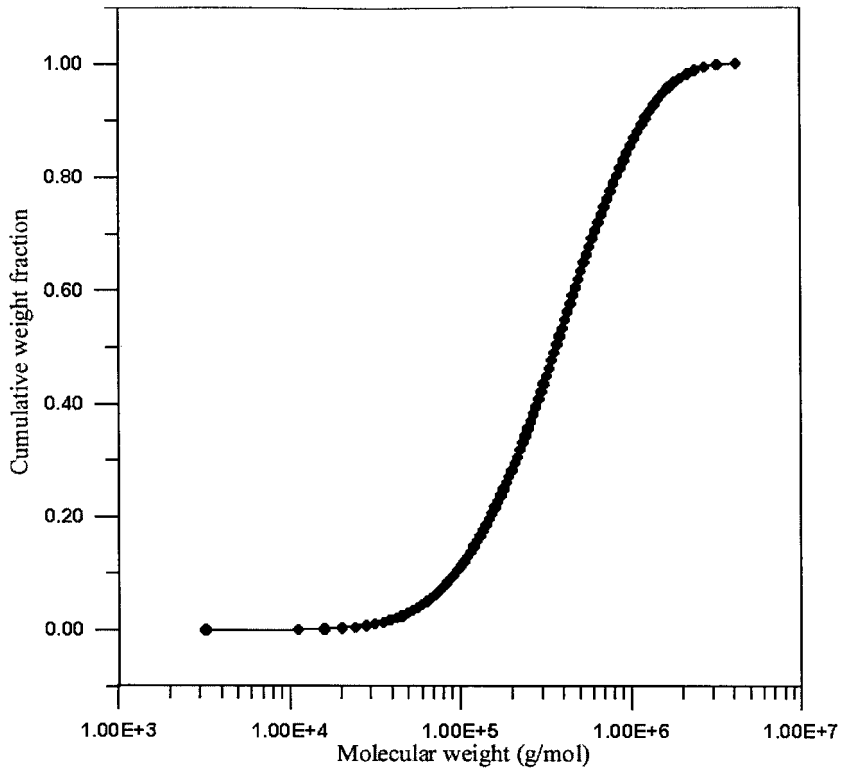

Figure 7 Deconvolution of the experimental MWD for polymerization H10, with the use of two catalyst sites. (●, experimental; —, model).

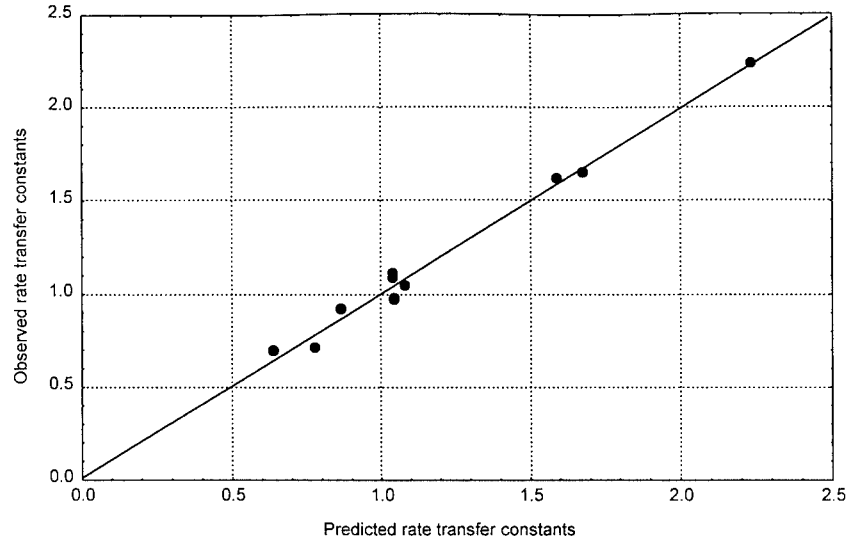

A)

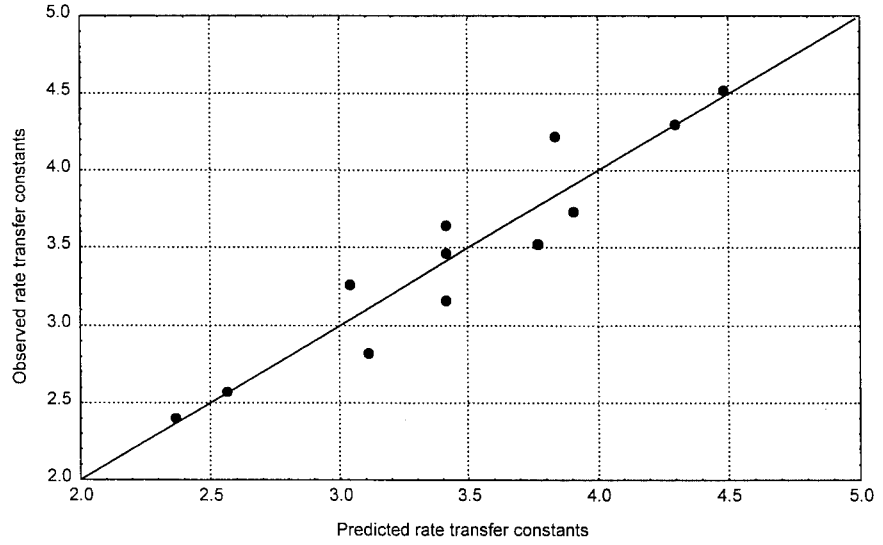

B)

Figure 8 Correlation between the predicted and the observed chain transfer constants to the site 1 (A) and site 2 (B).

lyst site type j, and F_L is the mass fraction of polymer chains with size smaller than or equal to L.

Equation (23) is the model used in this work to represent experimental MWD obtained by GPC. As mentioned previously,[10] the use of eq. (23) is very convenient. It is much easier to analyze model deviations and trends with the cumulative distribution because F_L is always a monotonic increasing function of i constrained in the interval [0, 1], which provides a natural normalization interval for all polymer samples. Besides, eq. (23) allows the manipulation of numbers of similar orders of magnitude, which enhances the performance of numerical procedures.

Observe that the model used here contains $(2N - 1)$ parameters to be determined: $q_1, \ldots, q_N, \ldots, a_1, \ldots, a_N - 1$, as $\Sigma_{j=1}^{N} \alpha_j = 1$. As polymer average molecular weights are large, parameters q_j are always very close to 1 and are not allowed to grow above 1 or decrease below 0. For these reasons, the parameters q_j are conveniently rewritten as:

$$q_j = \exp(-\theta_j) \tag{24}$$

In this work, the deconvolution problem consists of estimating the parameters $q_1, \ldots, q_N, \ldots, a_1, \ldots, a_{N-1}$ in eqs. (21)-(22) to reproduce experimental cumulative MWDs obtained through GPC. The estimation procedure, implemented in FORTRAN by using a standard library of maximum-likelihood parameter estimation routines,[25] is repeated iteratively for the increasing

TABLE IX
Ratios Between the Propagation and the Chain Transfer Reactions for Sites 1 and 2 (T = 65°C, x_H = 3.5 mol %, TEA = 55 ppm)

Value $\times 10^4$	Site 1	Site 2
Spontaneous or to monomer	0.194	2.379
Hydrogen	0.483	0.666
TEA	0.725	0.361

number of catalytic sites (N), until one (or both) of the following tolerance criteria is satisfied:[10]

1. The model obtained leads to a computed polydispersity index that is larger than the one obtained experimentally. This heuristic procedure assumes that increasing the number of catalyst site types will not cause narrowing of the computed MWD.

2. The partial activities of some of the catalyst site types are not statistically significant, as evaluated with the standard Student t-test.[26] If the additional parameters lead to a model that is not statistically significant, it is assumed that the additional site type is not relevant for the deconvolution of the experimental MWD.

Deconvolution of the total polymer GPCs

The number of active catalyst sites necessary to describe the total polymer MWD was equal to 2 in all experiments, except H6. The use of only one catalyst site invariably led to an inadequate description of the polymer molecular weight distribution (Figs. 6 and 7) and to a polydispersion index close to 2, much smaller than the polydispersion index of polymer samples analyzed. The use of one extra site (N = 3) led to insignificant partial activities, implying that this extra site was not necessary to describe the total polymer molecular weight distribution. Table VII presents the estimated parameters and Figures 6 and 7 show typical fitting results of the experimental GPC data.

When the correlation coefficients of q_1, q_2, and a_1 with the other independent and dependent variables presented previously are computed (Table VIII), it is found that the only significant correlations are the ones which relate the hydrogen fraction with the partial activities and transfer rates of the catalyst sites. In this case, the correlation coefficient between x_H and a_1 is equal to -0.63, which means that the higher the hydrogen pressure is, the higher the polymer weight fraction of polymer chains of low average molecular weight also is. Besides, the correlation coefficients between x_H and q_1 and q_2 are equal to 0.86, which means that the average molecular weight of the polymer produced in both catalyst sites decreases very significantly with the increase of the hydrogen concentration. Therefore, as the hydrogen concentration increases, the average molecular weight decreases significantly because the chain transfer rates increase in both sites and because the fraction of catalyst sites that produce polymer of lower molecular weights also increase. This cannot be explained by classical kinetic mechanisms, unless it is assumed that hydrogen plays an important role for activation of catalyst sites. As said before, this is in accordance with the current interpretation of the hydrogen effect on the propylene polymerization[27] as being caused by the reduction of the number of monomer-hindered growing chains due to transfer to hydrogen and the activation of new catalyst sites. Interestingly, the linear main effect analysis carried out using multiple linear regression leads to similar results for q_1 and q_2. However, it shows (Table VIII) that all independent experimental variables are important for the final fraction of polymer produced by each site (a_1), demonstrating the high complexity of this catalytic system.

A deeper analysis of the GPC data allows one to obtain the most significant chain transfer rate constants for the polymerization. The main hypotheses needed for parameter estimation are that the chain growth is not limited by catalyst deactivation, that catalyst sites keep their intrinsic kinetic behavior along the polymerization run, that reaction orders are equal to one in respect to all reactants, and that polymerization conditions remain constant. In this case, q_j can be described as:

$$q_j = \frac{Kp_j[M]}{Kp_j[M] + \sum_{i=1}^{NX} Ktr_{ij}[X_i]} \tag{25}$$

where Kp_j and Ktr_{ij} are, respectively, the kinetic constants for propagation and the kinetic constants for chain transfer with the chain transfer agent X_i. Therefore,

$$\frac{1}{q_j} - 1 = \exp(\theta_j) - 1 = \sum_{i=1}^{NX} \frac{Ktr_{ij}}{Kp_j}\frac{[X_i]}{[M]} \tag{26}$$

In the system analyzed, chain transfer is expected to occur to monomer, to hydrogen, and to cocatalyst and also to occur spontaneously. This means that at least four different kinetic constants (eight parameters) can be estimated simultaneously to describe the variations of q_1 and q_2 along the experimental grid. The strategy used here is similar to the strategy used previously to estimate q_j, although implemented in the reverse order. Parameters are estimated simultaneously by using the complete model and the least significant set of parameters is discarded. The model is then simplified and the estimation procedure is repeated. The iteration loop is halted when either all parameters are

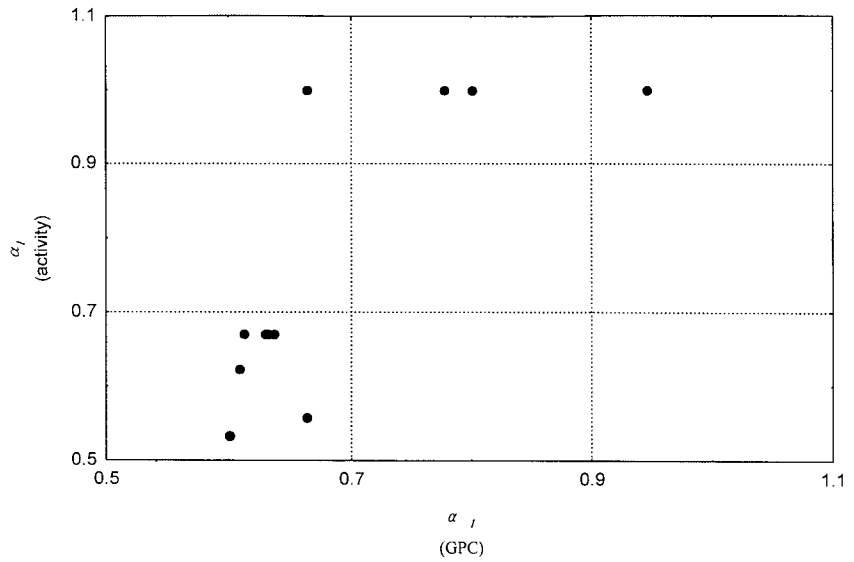

Figure 9 Correlation between the partial activities obtained by GPC and activity data [eq. (20)].

statistically significant or when a significant decrease of the correlation coefficient is observed (for instance, the correlation coefficient drops >10%). Results obtained are illustrated in eqs. (27)-(28) and in Figure 8(A, B):

$$\left(\frac{1}{q_1}-1\right)\times 10^4 = 0.2290\exp\left(23639.2\left(\frac{1}{T}-\frac{1}{338.15}\right)\right) + 0.4680\exp\left(-1722.9\left(\frac{1}{T}-\frac{1}{338.15}\right)\right)P_H + 0.0067\exp\left(-17265.2\left(\frac{1}{T}-\frac{1}{338.15}\right)\right)\mathrm{TEA} \quad (27)$$

with correlation coefficient equal to 0.99 and

$$\left(\frac{1}{q_2}-1\right)\times 10^4 = 2.4081\exp\left(125.6\left(\frac{1}{T}-\frac{1}{338.15}\right)\right) + 0.64672\exp\left(-10182.9\left(\frac{1}{T}-\frac{1}{338.15}\right)\right)P_H + 0.0052\exp\left(-18300.7\left(\frac{1}{T}-\frac{1}{338.15}\right)\right)\mathrm{TEA} \quad (28)$$

with correlation coefficient equal to 0.95. Pressures are given in atm and concentrations are given in ppm. As partial pressures are used to replace concentrations, it is implicitly assumed that Henry's law is valid and that the Henry coefficient is essentially constant in the experimental range analyzed. Both assumptions can be relaxed if more rigorous computation of monomer and hydrogen solubilities are required. However, these assumptions are believed to be very good in the cases analyzed, given the narrow temperature ranges used experimentally.[15]

Equations (27) and (28) indicate that chain growth is controlled by chain transfer to hydrogen, to monomer (or spontaneous), and to TEA in both sites, whereas the chain transfer to monomer (or spontaneous) is significantly higher in site 2. These effects are the usual chain transfer effects reported in the literature for the catalyst studied.[15,16] Table IX shows the importance of the chain-transfer effects at the center of the experimental grid for each site.

After estimating the chain transfer constants for each site, it is important to reconcile the partial activities calculated for each site from the GPC and the productivity data. The fraction of polymer produced at the catalyst site 1 may be described as:

$$\alpha_1 = \frac{K_{P1}Mcat_1}{K_{P1}Mcat_1 + K_{P2}Mcat_2} = \frac{K_{P1}Mcat_1}{K_pMcat} \quad (29)$$

that is valid if the polymerization conditions are kept constant, the activation/deactivation characteristics of both sites are similar, and there is no site transformation throughout the polymerization. Analyzing eq. (29), it is not difficult to notice that it is impossible to estimate the fraction of sites type 1 and the individual propagation constant of this site simultaneously, as discussed previously.[10] As implemented before, the fraction of site type 1 is defined *a priori* and afterwards the propagation rate constant is estimated.

Partial activities were obtained for productivity data and GPC. It is important to verify if there is any significant correlation between these quantities. Figure 9 shows the fraction of sites 1 predicted from productivity and GPC data. There is no clear correlation between them and they definitively do not represent the same experimental variable. That is not sur-

TABLE X
Parameters of the Partial Polymer Yield for Each Catalyst Site

	Site 1	Site 2
A	0.677	9.78
E_A	1201.3	4365.1
k_d	2.126	1.053
Kx_{i1}^a	2.464	1.112
Kx_{i2}^a	1.602	1.326
Kx_{i3}^a	0.928	1.776
Kx_{i4}^a	2.405	1.326
r^2	0.93	0.95

prising, as even in the absence of hydrogen, there are two different polymer families produced solely by the sites activated by cocatalysts (e.g., experiment H1). Thus, one has to admit that both sites activated by hydrogen and cocatalysts can produce high molecular weight and low molecular weight families of polymer. Therefore, cocatalysts and hydrogen activate both the site that produces low molecular weight polymer chains (1) and the site that produces high molecular polymer (2) chains.

The chain transfer rate constants for the two families of catalyst sites (that produce short and long polymer chains) are presented in eqs. (27)-(28). The partial activities of these sites should be revised. Our goal is to make the partial activities of the sites activated by hydrogen and cocatalyst calculated from GPC data agree with the ones calculated from productivity data and vice versa. This is possible if

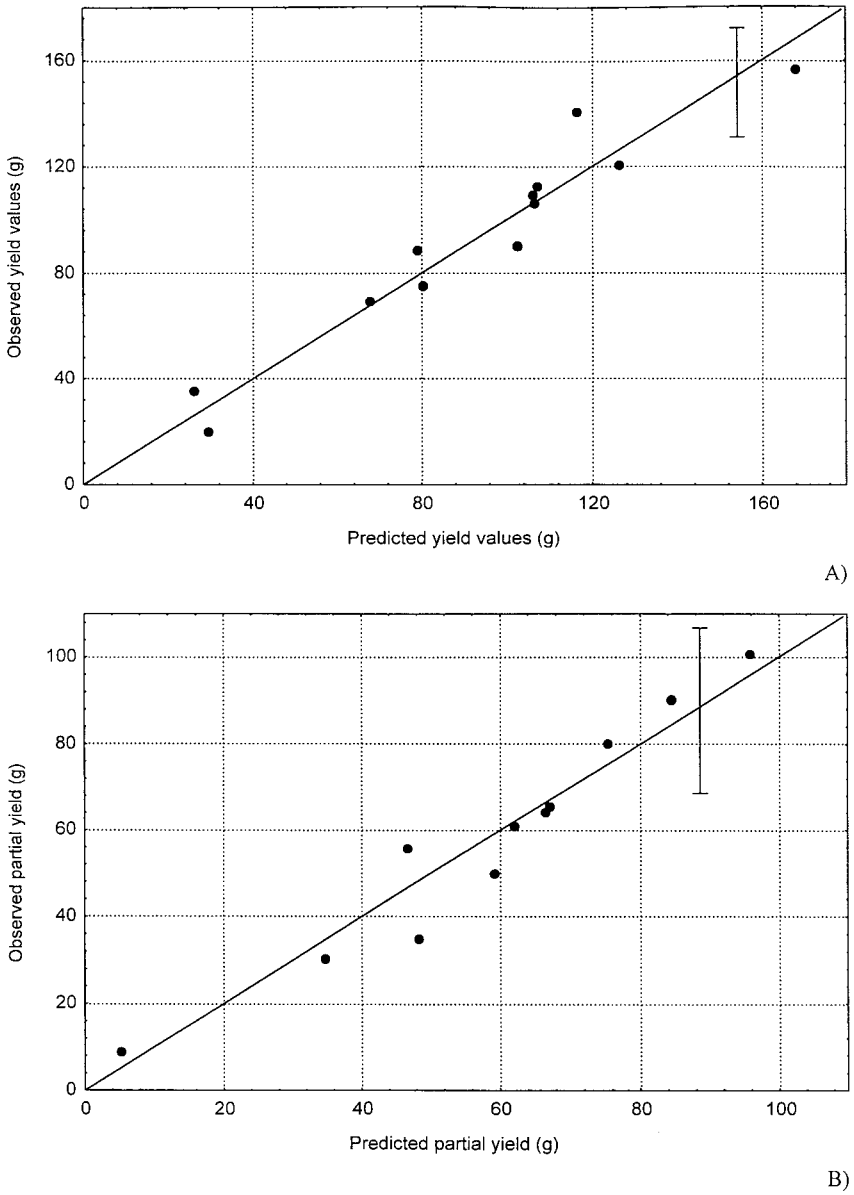

Figure 10 Observed and predicted polymerization yields [eq. (31)] for site 1 (A) and site 2 (B).

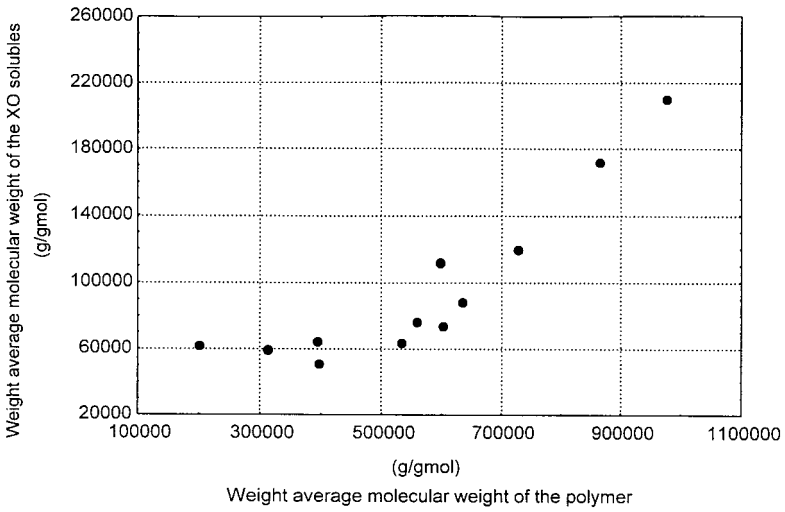

Figure 11 Correlation between the average weight molecular weight of the total polymer and the soluble fraction.

$$P_k = P\alpha_k^{\mathrm{GPC}} \tag{30}$$

where P_k is the partial yield of site k, P is the total yield, and α_k^{GPC} is the fraction of polymer produced by site k. The partial activities are then calculated for each experiment with the help of eq. (30) and the experimental polymer yield data. The "pseudoexperimental" partial activity data are then modeled as presented in eq. (20). Parameters obtained are presented in Table X. It should be noted that the parameter effectively estimated in eq. (30) is $e^{A}Kx_{ij}^{a}$, where the superscript a refers to the partial activity model:

$$P_i = \frac{e^{[A_i-(E_{A_i}/T)]}}{K_{d_i}}(1 - e^{-K_{d,1}})(Kx_{i1}^{a}\sqrt{\mathrm{DEAC}} + Kx_{i2}^{a}\sqrt{\mathrm{TEA}} + Kx_{i3}^{a}\sqrt{H_2} - Kx_{i4}^{a}\sqrt{\mathrm{PEEB}})pM\,Mcat \tag{31}$$

At experiment H6 (Table VII), in which the MWD of the polymer produced could not be deconvoluted into their individual Flory distributions, it was assumed for parameter estimation purposes that both sites contributed to the same extent to final MWD. Figure 10 shows the correlation between the calculated polymerization yield for each catalytic site and the experimental yield.

Analysis of the XO fraction

The XO fraction is an atactic-rich polymer fraction, although it also contains certain amounts of isotactic chains of lower molecular weights. The XO fraction is obtained through fractionation of total polymer and the proper understanding of the quality of the XO fraction to involve both the kinetics of polymerization and the equilibrium/kinetics of polymer chain extraction by boiling xylene. A detailed investigation of the extraction phenomena is beyond the scope of this article; however, it is important for process study purposes to understand the factors that may influence on the XO amount.

Figure 11 presents the relation between the weight-average molecular weight of the XO fraction and of the total polymer. It is possible to observe that the average molecular weight decreases as the polymer molecular weight decreases, until an inferior limit is reached. This limit is probably associated with thermodynamic considerations related to the material solubility. Even though there is no theoretical foundation for the use of the Schulz–Flory for the deconvolution of the GPC curves obtained for the XO fraction, it was possible to obtain a very good fitting (Fig. 12) by using a two-site distribution (the parameters obtained are shown in Table XI). Figure 12 presents the MWD of

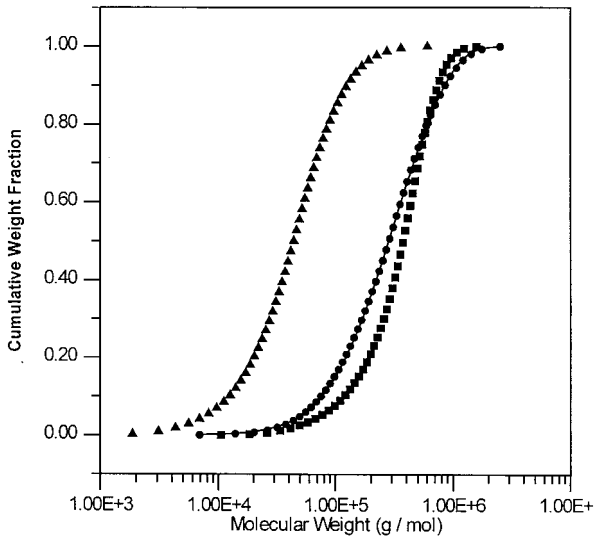

Figure 12 Cumulative MWD distribution for the total polymer (●, experimental; —, model), insoluble fraction (■), and XO soluble fraction (▲) in experiment H3.

TABLE XI
Deconvolution of the MWD of the XO Fractions

Label	θ_1	θ_2	α_1	PM_n (g/gmol)	PM_w (g/gmol)	PD
H1	1.839×10^{-4}	8.218×10^{-4}	0.1967	81,400	172,000	2.11
H2	2.848×10^{-4}	10.12×10^{-4}	0.1693	58,600	119,000	2.03
H3	8.512×10^{-4}	20.59×10^{-4}	0.1648	25,200	50,300	2.00
H4	5.513×10^{-4}	16.91×10^{-4}	0.1397	32,000	64,000	2.00
H5	3.986×10^{-4}	14.98×10^{-4}	0.0214	29,700	59,400	2.00
H6	6.440×10^{-4}	16.54×10^{-4}	0.1380	30,900	61,800	2.00
H7	3.001×10^{-4}	10.49×10^{-4}	0.1598	55,300	112,000	2.02
H8	1.764×10^{-4}	5.96×10^{-4}	0.2064	100,100	210,000	2.10
H9	4.369×10^{-4}	12.89×10^{-4}	0.0868	38,100	76,200	2.00
H11	4.546×10^{-4}	13.18×10^{-4}	0.0828	36,900	73,800	2.00
H12	3.841×10^{-4}	12.20×10^{-4}	0.1254	43,700	87,600	2.01

the xylene-soluble and -insoluble fractions, as well as the MWD of the total polymer. It can be noted that the total polymer MWD is very similar to the insoluble polymer curve except to the lower molecular weight portion of the curve that is present on the XO curve. This seems to indicate that part of the isotactic propylene is indeed removed by xylene during extraction.

Interpretation of NMR spectra

The model used for interpretation of NMR spectra and parameter estimation is presented in detail in the previous study.[10] Over the experimental range investigated, the polymer microstructure was fairly constant compared to the experimental error (±2%), which is relatively common, especially when the experimental range analyzed is narrow.[10] This means that the relative amounts of atactic and isotactic catalyst sites are subject to much larger fluctuations in the experimental range analyzed than the kinetic constants for specific monomer chain insertions. Typical NMR spectra for both overall and XO polymer samples are shown in Figure 13. Figure 14 shows the polymer microstructure for selected experiments and the calculated polymer microstructure assuming that the catalyst stereoselectivity can be described by a site-control mechanism with an average stereoselectivity of 0.968.

Simulation of actual industrial operation conditions

The parameter estimates were used to simulate the steady-state response of bulk PP polymerization in a single continuous stirred tank reactor (CSTR) (the well known LIPP technology), using the previously described high-activity fourth-generation Ziegler–Natta catalysts. In the LIPP technology, a single reactor is used to produce the PP, so that feed lines to other reactors do not exist. Besides, no diluent is fed into the reactor vessel and the solid powder is suspended in a monomer liquid phase. Polymerization heat is removed by condensation of boiling propylene. Mono-

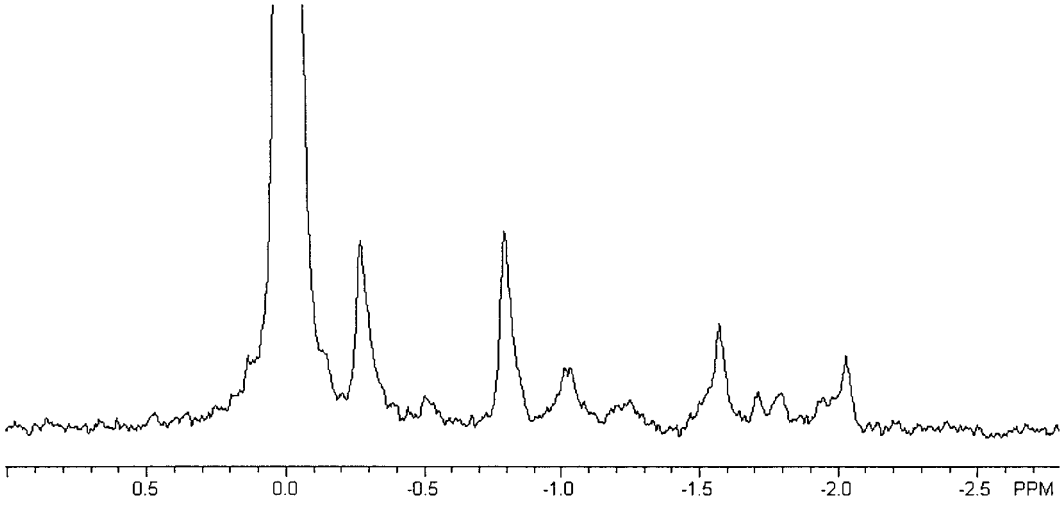

Figure 13 Typical polypropylene ^{13}C-NMR spectra in the methyl region (Experiment H2, and the *mmmm* pentad was used as reference).

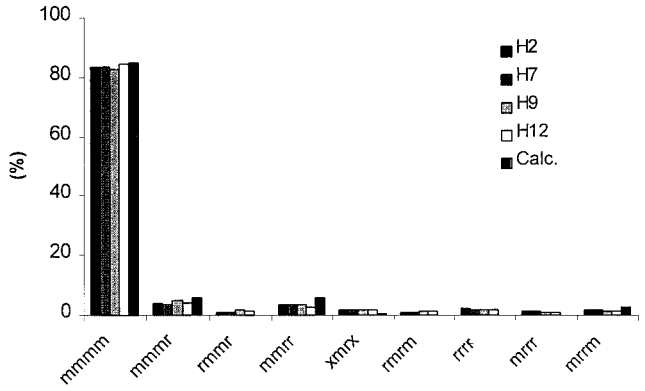

Figure 14 Pentad analysis for selected experiment and model fit for them.

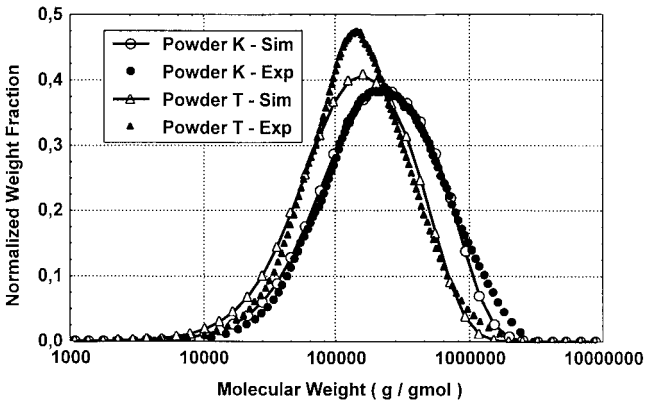

Figure 15 MWD of the polymer powder–LIPP homopolymerization.

mer feed rates are usually limited by the maximum solid hold-up to keep the suspension stable. The MWD is controlled with the hydrogen feed stream and operation pressures are around 30 atm. Important issues for this technology are the control of solid hold-up of liquid propane concentration and of XO. Increase of XO indicates poor control of the degree of isotacticity. Variations of liquid propane concentration may prejudice polymer productivity and cause modification of the quality of the final resin. There are about 20 plants worldwide producing PP with this technology. Typical bulk plant capacity is around 160,000 ton PP/year. It is important to emphasize that process data shown below were not used for parameter estimation and model building. All simulation modules and data banks were built independently. Detailed presentation of the process model is presented elsewhere.[28]

Table XII shows gas-phase compositions obtained at plant site and with the model. Agreement is quite fair. Figure 15 shows the MWD of two polymer grades compared to the MWD predicted by the model. Once more, results may be regarded as very good. Other key process variables, such as the XO (experimental value is equal to 3.60, while simulation value is equal to 3.77), the degree of isotacticity (experimental and simulated values are equal to 0.97), and the fraction of isotactic pentads (experimental and simulated values are equal to 0.92), are described very well by the model. Therefore, it may be said that the model parameters are able to represent very successfully the slurry PP homopolymerization performed in accordance with the LIPP technology.

CONCLUSIONS

A method was presented for kinetic characterization of catalysts for olefin polymerizations, to allow the estimation of kinetic parameters for use in process simulators. The method allowed the successful characterization of fourth-generation Ziegler–Natta catalysts for bulk propylene polymerizations with relatively few experiments. The total number of experiments performed was equal to 24, corresponding to 13 different experimental conditions, as replicates were carried out to assure the consistency of the experimental results. Eleven experimental conditions were used for main-effect analysis and two additional experimental conditions were used for analyzing the catalyst decay. The experiments allowed the evaluation of the effects caused by seven independent variables upon the final polymerization results. The method presented here does not depend on the evaluation of polymerization rate profiles and relies on the availability of overall polymer yields, GPC chromatograms, and NMR spectra of polymer samples. As the number of proposed experiments is relatively small and the techniques used for polymer characterization are rather standard, the method can be very easily implemented at plant site and encourages the use of process simulators for actual process studies.

TABLE XII
Experimental and Simulation Gas-Phase Compositions (molar %) for Different Operation Conditions—LIPP Homopolymerization

Powder	Propene (Exp.)	Propane (Exp.)	H_2 (Exp.)	MI (Exp.)	Propene (Calc.)	Propane (Calc.)	H_2 (Calc.)	MI (Calc.)
K	85.3	11.8	3.05	3–4	85.0	12.0	2.94	4.1
T	82.8	9.40	7.35	15–17	82.0	11.0	7.00	15.5

It was shown that chain transfer to hydrogen controls the molecular weight distribution of the final polymer obtained with the catalyst analyzed. The method allowed the detection of important hydrogen and cocatalyst effects upon the catalyst activity, catalyst stability, and molecular weight distribution of the polymer product. It was observed for this catalyst that the increase of the hydrogen concentration exerts a pronounced effect upon the catalyst activity of sites that produce material of low molecular weight, so that the average polymer molecular weight decreases with order greater than 1 when the hydrogen concentration increases. Additionally, it was shown that the internal stereo-block configuration of polymer chains is not sensitive to changes of the polymerization conditions in the range analyzed, so that the catalyst performance at the stereo-block level is essentially constant.

The kinetic parameters estimated with the help of simple kinetic models were inserted into a process simulator and allowed the proper description of plant operation. Therefore, the consistent set of parameters presented here may be used as a benchmark for simulation studies of bulk propylene polymerizations and as initial guesses for development of more complex kinetic models.

The authors thank Polibrasil Resinas SA for supporting this project. M.N.S. and J.C.P. thank CNPq for providing scholarships. The authors are also indebted to all engineers of Polibrasil for valuable discussions and sound advice. The authors also thank Prof. Maria Inês Bruno, from Instituto de Macromoléculas, Universidade Federal do Rio de Janeiro, for the NMR characterization of polymer samples.

References

1. Moore, E. P., Jr. (Ed.). Polypropylene Handbook: Polymerization Characterization, Properties, Processing Applications; Hanser Gardner Publications: New York, 1996.
2. Chemical and Engineering News 2000, 78, 20.
3. Pinto, J. C.; SIMULPOL 3.0—Software for Simulation of Slurry and Bulk Propylene Polymerizations; The User's Guide, Internal Report, Polibrasil Resinas SA, Camaçari-BA, 1999.
4. Zabisky, R. C. M.; Chan, W.-M.; Gloor, P. E.; Hamielec, A. E. Polymer 1992, 33, 2243.
5. Soares, J. B. P.; Hamielec, A. E. Polym React Eng 1996, 4, 153.
6. Xie, T.; McAuley, K. B.; Hsu, J. C. C.; Bacon, D. W.; Ind Eng Chem Res 1994, 33, 449–479.
7. Zacca, J. J.; Debling, J. A.; Ray, W. H. Chem Eng Sci 1996, 51, 4859–4886.
8. Nele, M.; Pinto, J.C. J Appl Polym Sci 1997, 35, 1403–1413.
9. der Ven, S. V. Polypropylene and Other Polyolefins: Polymerization and Characterization; Elsevier Science: Amsterdam, 1990.
10 Matos, V.; Mattos Neto, A. G.; Pinto, J. C. J Appl Polym Sci 2001, 79, 2076.
11. Zacca, J. J.; Ray, W. H. Chem Eng Sci 1993, 48, 3743–3765.
12. Sarkar, P.; Gupta, S. K. Polym Eng Sci 1992, 32, 732–742.
13. Samson, J. J. C.; Weickert, G.; Heerze, A. E.; Westerterp, K. R. AICHE J 1998, 44, 1424–1437.
14. Samson, J. J. C.; Bosman, P. J.; Weickert, G.; Westerterp, K. R. J Polym Sci, Part A: Polym Chem 1999, 37, 219–232.
15. Guinot, P.; Othman, N.; Fevotte, G.; McKenna, T. F. Polym React Eng 2000, 8, 115–134.
16. Tonelli, A. E. NMR Spectroscopy and Polymer Microstructure: The Conformational Connection; VCH: New York, 1991.
17. Phan, Q.; Petiaud, R.; Waton, H.; Darricades, M. F. L. Proton and Carbon NMR Spectra of Polymers; Penton Press: London, 1991.
18. Mori, H.; Endo, M.; Tashino, K.; Terano, M. J. Mol Catal A Chem 1999, 145, 153–158.
19. Soares, J. B. P.; Hamielec, A. E. Polymer 1996, 37, 4599–4605.
20. Keii, T. Kinetics of Ziegler–Natta Polymerization; Kodansha Scientific Books: Tokyo, 1972.
21. Kim, I.; Choi, H. K.; Kim, J. H., Woo, S. I. J Polym Sci, Part A: Polym Chem 1994, 32, 971–977.
22. Ross, P. J. Taguchi Techniques for Quality Engineering, 2nd ed.; McGraw-Hill: New York, 1996.
23. Shaffer, W. K. A.; Ray, W. H. J Appl Polym Sci 1997, 65, 1053–1080.
24. Froment, G. F.; Bischoff, K. B. Chemical Reactor Analysis and Design, 2nd ed., Wiley: New York, 1990.
25. Pinto, J. C. ESTIMA—A Software for Parameter Estimation and Experimental Design, User's Guide; PEQ/COPPE/UFRJ: Rio de Janeiro, 1999.
26. Box, W.; Hunter, J. S.; Hunter, W. G. Statistics for Experimenters: An Introduction to Design, Data Analysis, and Model Building; Wiley: New York, 1978.
27. Alman, E. J.; Cossee, P. J Catal 1960, 3, 99.
28. Mattos Neto, A. G.; Pinto, J. C. Chem Eng Sci 2001, 56, 4043–4057.